Chapter 5

Tagging spectrometer

5.1   Specifications and introduction

To satisfy the needs of the GLUEX physics program, the tagged photon spectrometer should meet the following specifications:

1. Photon energy detection from 70% to 75% of E_0 with energy resolution of about 0.1% r.m.s. Percentages refer to the primary beam energy E_0, i.e. for a $12GeV$ beam an energy resolution of $12MeV$ is needed for photons between 8.4 and $9GeV$.

2. A detector system which allows a counting rate of at least 5×10^6 electrons per second per 0.1% over this range of photon energies.

3. An additional capability for photon energy detection from 25% to 90% of E_0 (3 to 10.8 GeV if E$_0$=12 GeV), with less stringent resolution and count rate requirements.

4. A quadrupole magnet between the radiator and dipole spectrometer which images the beam spot on the radiator onto a line on the focal plane. This feature makes it possible to envision the use of focal plane counters with two-dimensional readout, with which one could enhance the tagging efficiency of the source. Focal plane detectors with two-dimensional readout are considered as a possible upgrade beyond the baseline design presented in this chapter. Any improvements obtained using this technique would be over and above the performance figures presented in this report.
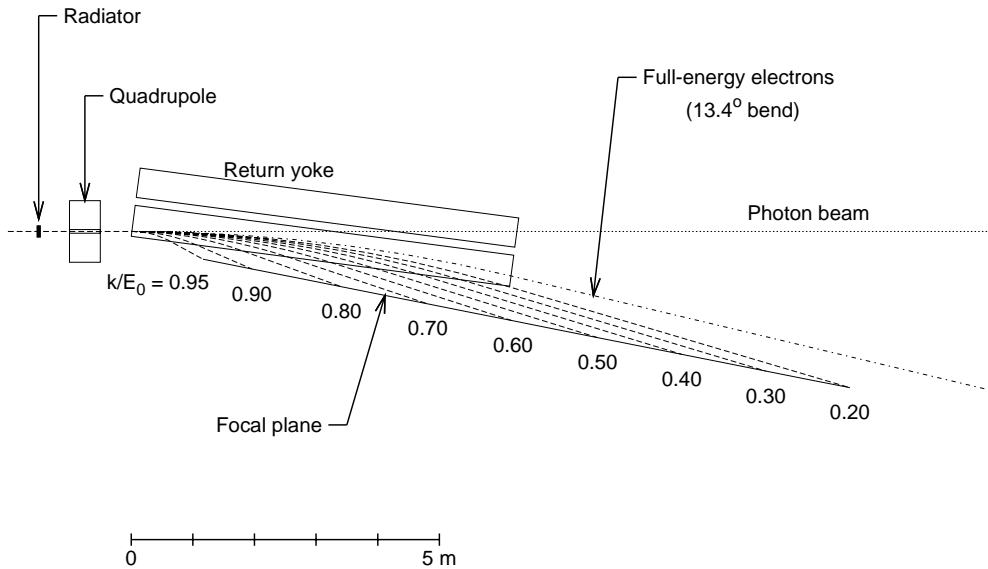
Figure 5.1: A plan view of the tagging spectrometer from above, showing the path of the primary beam and the trajectory of post-bremsstrahlung electrons of various recoil momenta.

The system described below, based on a room-temperature design, meets all of these criteria. The option of a superconducting design was also studied. With a superconducting magnet, the spectrometer could operate at much higher fields, offering the possibility of some space savings in the size of the tagger focal plane array. An iron yoke design was found which would clamp the 5 T field sufficiently to make it possible to operate normal phototubes on the nearby tagger focal plane. However, as shown below, rate considerations require a degree of segmentation in the tagging counters such that it is impractical to increase the dispersion along the focal plane above what is provided by a 1.5 T room temperature magnet. Given that there was no liquid helium available in the tagger hall, the savings in electrical power did not justify the additional cost and complexity of a superconducting magnet.

The tagging spectrometer is an Elbek-type spectrometer and is shown schematically in Figure 5.1. The 12 GeV electrons pass through the radia-

tor target where a small fraction undergo a bremsstrahlung interaction. The electrons then pass through a focusing quadrupole and are bent by the 6.3 m long tagger magnet. The majority of the electrons which did not interact with the radiator are bent by 13.4° and then propagate straight to the electron beam dump. A large vacuum vessel is integrated into the magnet and extends out to the spectrometer focal plane so only the small amount of multiple scattering inside the diamond radiator and in the exit window effect the resolution. The spectrometer detectors are positioned immediately outside the focal plane.

The detector package is divided into two parts: a set of 190 fixed scintillation counters spanning the electron momentum range from 0.6 to 9 GeV, and a movable "microscope" of 500 scintillating fibers optimized for normal operation spanning the energy range from 8.4 to 9 GeV.

The fixed array provides access to the full tagged photon spectrum, albeit at a modest energy resolution of 0.5% and reduced photon spectral intensity. These detectors are well suited for running with a broadband incoherent bremsstrahlung source. They enable experiments to be performed with the highest photon energies possible with the source. When running with a coherent source they play an essential role in the crystal alignment procedure, and provide a continuous monitor of the performance of the source. The microscope is needed in order to run the source in coherent mode at the highest polarization and intensities, and whenever energy resolution better than 0.5% is required. Using the microscope, the source is capable of producing photon spectral intensities in excess of 2×10^8 photons/GeV, although accidental tagging rates will limit normal operation to somewhat less than this.

5.2 Magnet

The tagger magnet (Fig. 5.2) is similar to the existing tagger magnet in Hall B of Jefferson Lab [15]. The higher energy of the HALL D beam is largely compensated for by going to smaller bend angles, so the sizes of the magnets are comparable, and much of the experience from Hall B can be carried over. Unlike the Hall B tagger, which bends vertically, the HALL D tagger will deflect electrons in the horizontal plane, with both the detector hall and the beam dump constructed above ground.

The main parameters of the magnet are given in Table 5.1 and a cross sectional view is shown in Figure 5.2. The magnet is 1.13 m wide 1.41 m high and 6.3 m long and weighs a total of 80 metric tons. The pole tips are 470 mm wide 6.2 m long with a gap of 30 mm. The nominal operating field is 1.5 T though the coils are designed to operate at enough current for 1.8 T.
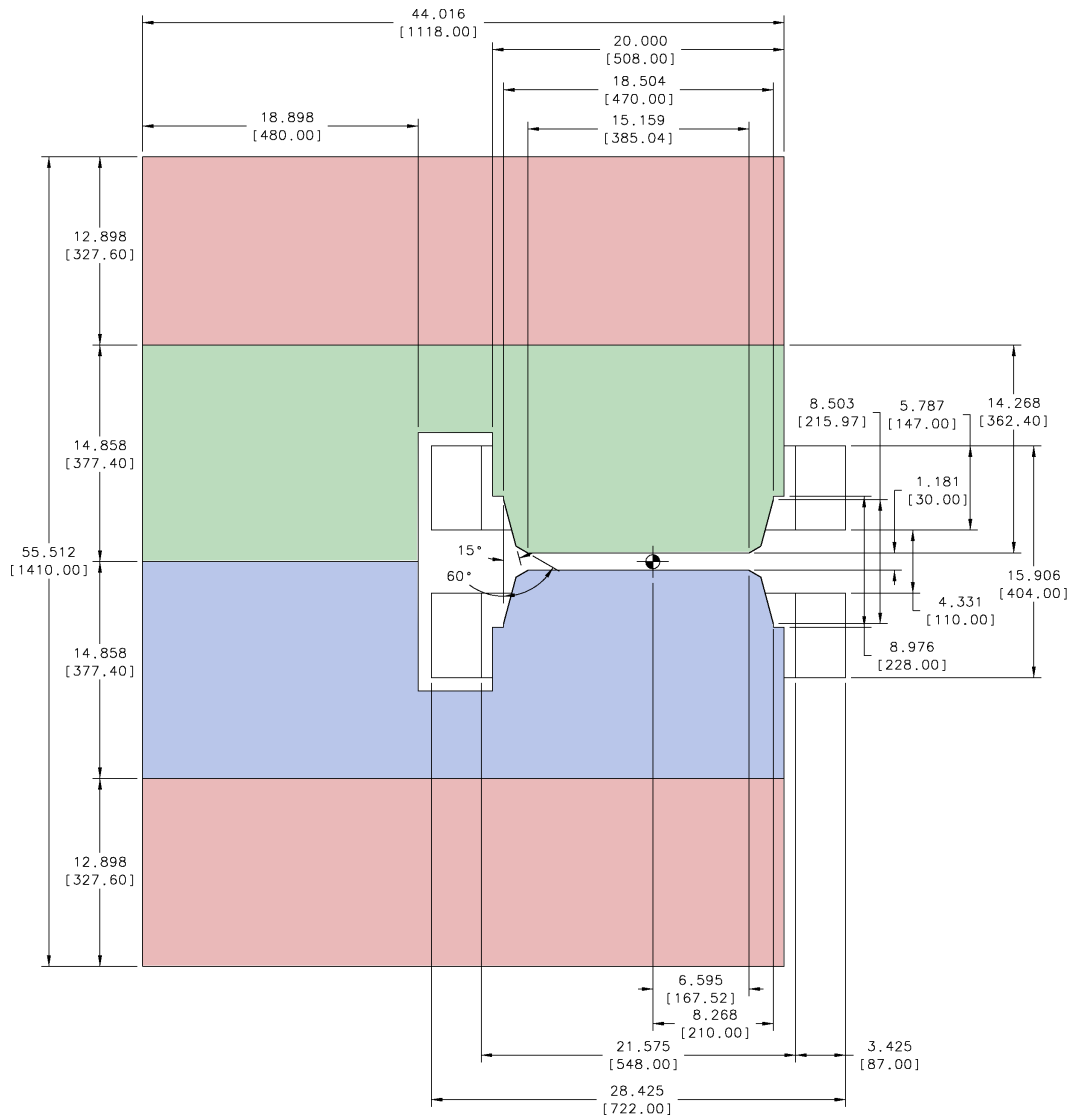
Figure 5.2: A section view of the tagging spectrometer's dipole magnet. The magnet is constructed of four 6.3 m long iron slabs. The two water cooled copper coils are shown but not the vacuum chamber. Dimensions are inches [mm].

Radius of curvature	26.7 m
Full-energy deflection	13.4^O
Field at 12 GeV	1.5 Tesla
Gap width	3.0 cm
Length of pole	6.3 m
Weight	80 tons
Length of focal plane (25% to 97% of E_0)	10.1 m
Coil power	220 A at 105 V

Table 5.1: Design parameters for the tagging spectrometer dipole magnet

At 1.5 T, the magnetic field inhomogeneity should be less than 1 part in 10^4 along any 100 mm length lying inside an area defined by the root of the pole stem. Within this area the maximum variation in the magnetic field should be less than 1 percent. To achieve this the pole faces must be parallel such that the variation in the pole gap is less than 0.02 mm along any 100 mm length on a pole surface. The variation in gap size should be less than 0.2 mm over the complete area of the poles. The variation in the pole gap between zero field and a field of 1.5 T should be less than 0.2 mm at any point on the vacuum chamber sealing surface. The magnet is constructed of four iron pieces which are bolted and pinned together. The maximum weight of a single piece is 25 t.

At the previous review in December 2006 a two magnet design was presented. Recently the advantages of a one magnet versus a two magnet design were investigated. In the present design the weight of the individual pieces is the same as in the previous two magnet design. Therefore the infrastructure for assembling the magnet is the same for both options. The raw material to manufacture the 6.3 m long magnet is available and several companies have facilities to manufacture these components. Detailed inquires into known magnet manufacturers indicated that only minimal cost difference existed between the two designs. The single magnet design has several performance advantages over the two magnet design. With a single magnet one does not have to align the two magnets to each other. This simplifies the magnet support and reduces the risk of vacuum leaks at the o-ring seal between the vacuum chamber and pole tip. Each pole tip will be made from a single piece of iron which will minimize variations in the magnetic field along the length of the magnet coming from chemical variations in the iron. The pole tip can be machined at the same time as the return yoke's horizontal plane. Therefore, the surfaces which define the poles relative alignment can be machined at the same time the pole
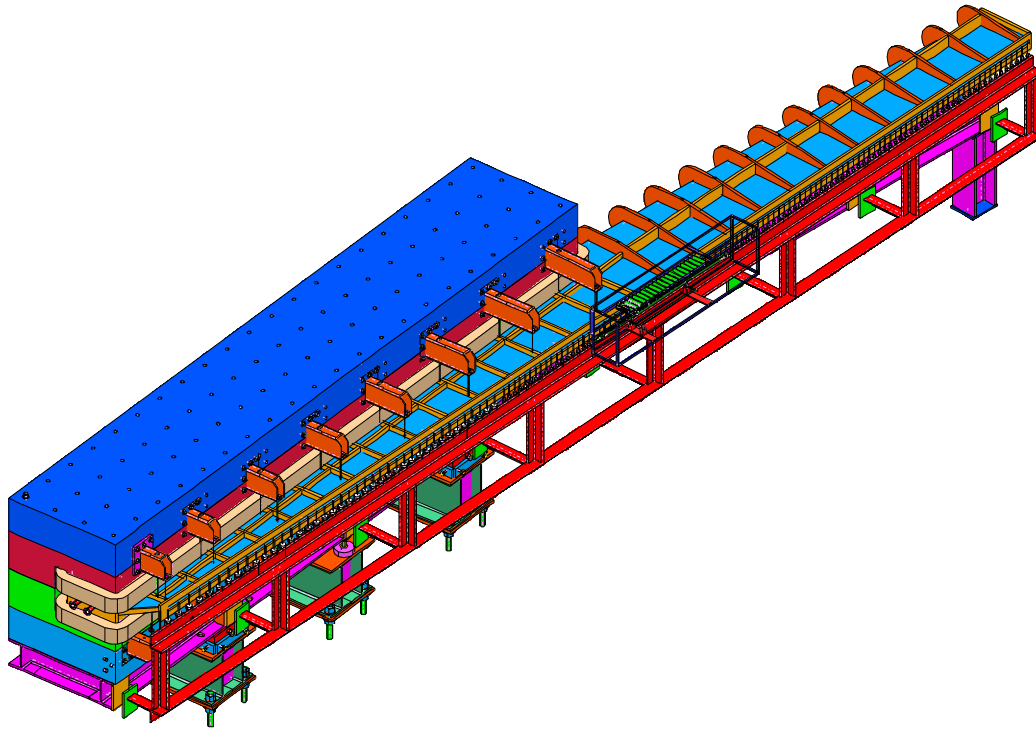
Figure 5.3: A 3-D model of the HALL D tagging spectrometer. The dipole magnet with the integrated vacuum chamber is shown. The magnet is supported with a 3 point adjustable support. Also shown in this figure are the fixed hodoscope array and the microscope detector package.

is machined, resulting in the best relative alignment possible. The alignment of the vacuum chamber is also simplified as there are only two sealing surfaces. Based on this it was decided to go back to the one magnet design.

The complete assembly of the magnet an vacuum chamber with the detector packages is shown in Figure 5.3. The magnet will be supported and adjusted from 3 points underneath. The deflection of the magnet due to it's own weight with this support is less than 25μm. The adjustment hardware consists of wedges that allow ±9 mm of adjustment in the vertical direction. In the horizontal plane, adjustment capability will be ±1 cm. This will easily compensate for the 1 inch maximum differential settling of the tagger hall and HALL D. Feducial marks will be provided for alignment on the iron yoke and transfer measurements performed to exactly measure the location of the feducials relative to the pole tips. Both hand calculations and a finite element
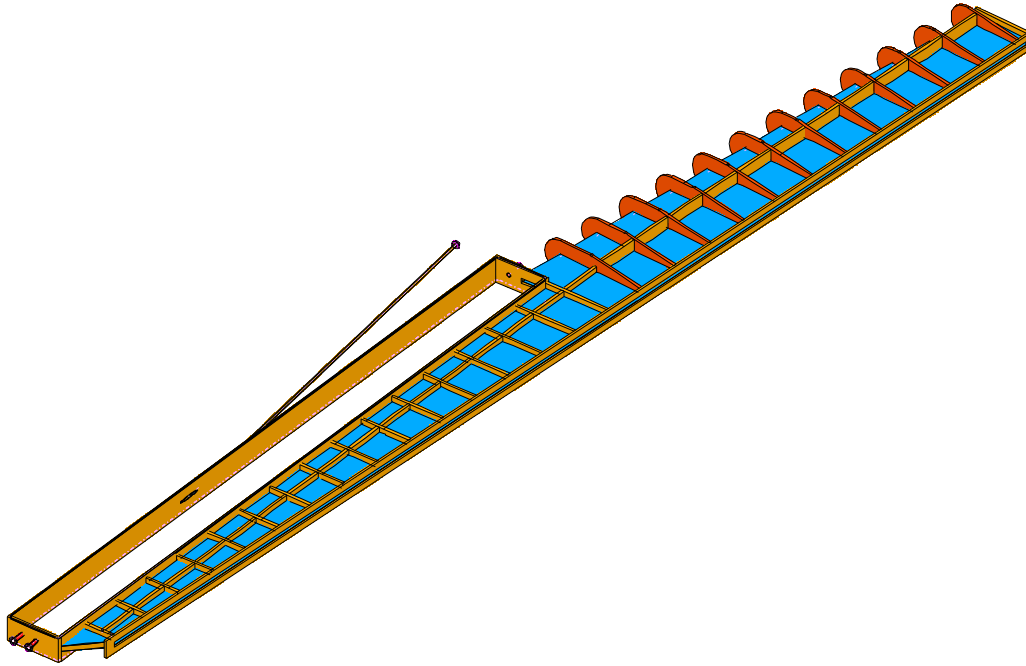
Figure 5.4: A 3-D model of the HALL D tagging spectrometer's vacuum chamber.

simulations estimated the magnetic force between the poles to be about 240 tonnes[16]. This is much more than the vacuum forces on which are about 75 tonnes. The magnetic force must be carried by the bolts which hold the iron plates together. An array of 1.5" (3.8 cm) bolts spaced every 12" (30 cm) which are installed under predefined load are sufficient to keep the assembly under tension. With this construction the total deflection of the poles under full load is about 0.1 mm. In this design 16 brackets are used to support the vacuum chamber from the magnet yoke.

The vacuum chamber for the tagging spectrometer is shown in Figure 5.4. The vacuum chamber is constructed with a 1/4" stainless steel shell and 1" reinforcing ribs. Maximum deflection of anywhere in the chamber is limited to 2.5 mm. Since the nominal opening in the chamber is 45 mm and only 30 mm is required, this is acceptable. The flange for the 11 m long exit window is 1" thick. The frame running around the pole tips is constructed of $1 - 1/4$" and 3/4" Stn.Stl. plate. The plan to use o-rings to seal the vacuum chamber to the poles has been explored.

Radiation levels are assumed to be low enough to not degrade the elasticity

of the o-rings for several decades. A 3/8 inch (9.5 mm) diameter viton o-rings of Shore A hardness of 70 will be used. In order to compress this o-ring to nominally 25%, 27,000 lbs will be required. The weight of the magnet alone will be sufficient to compress the o-ring. The tolerances on the machined parts are designed to ensure there is a minimum of 20% and a maximum of 30% compression in the o-ring. This will ensure vacuum integrity is maintained. The downstream photon beamline is 1" in diameter and ends in a standard conflat flange. The exit window will be constructed of thin aluminum foil. The downstream end of the vacuum chamber is still being designed. The design will be determined based on background in the fixed hodoscope array and the microscope.

The magnet will be assembled in place in the tagger hall. 12.5 t lifting eyes in the hall ceiling in the entry allow the pieces to be lifted from a truck and placed on rollers on the floor. Two lifting eyes will be used to lift each section. The pieces are moved next to the stand where a fixed crane will pick them up and stack them on the magnet stand. Care must be taken with the vacuum chamber; spacer blocks must be inserted in the chamber gap to support the 27,000 lbs load caused by the o-ring compression. As the weight of one of the iron plates is roughly the force needed to compress the o-ring no additional clamping is needed for this. The spacer blocks can be removed after the support brackets are installed.

5.3   Spectrometer optics

The optical properties of the tagging were optimized using the TRANSPORT program. For this and all other simulation in this section the CEBAF 12 GeV electron beam design goal parameters which were summarized in Table 4.1 were used. The setup of the TRANSPORT simulation is shown in Figure 5.5. A hard edge approximation was used for the fringe fields in this simulation and a magnetic field of 1.5 T in the high field region. If the input edge of the magnet is not perpendicular to the electron beam the entrance to the magnetic field will act as a lens. However the focal length associated with realistic entrance angle is much longer than the the total drift distance so this effect is not important for this design. Therefore it is assumed in these studies that the pole tips are rectangular. The remaining free parameters then are the distance between where the electrons enter the magnetic field and the outer corner of the field (I-B in Figure 5.5) and the and the angle between the output edge of the magnet and the original electron beam axis (this is the rotation angle of the magnet). A solution was sought which provided the optimum
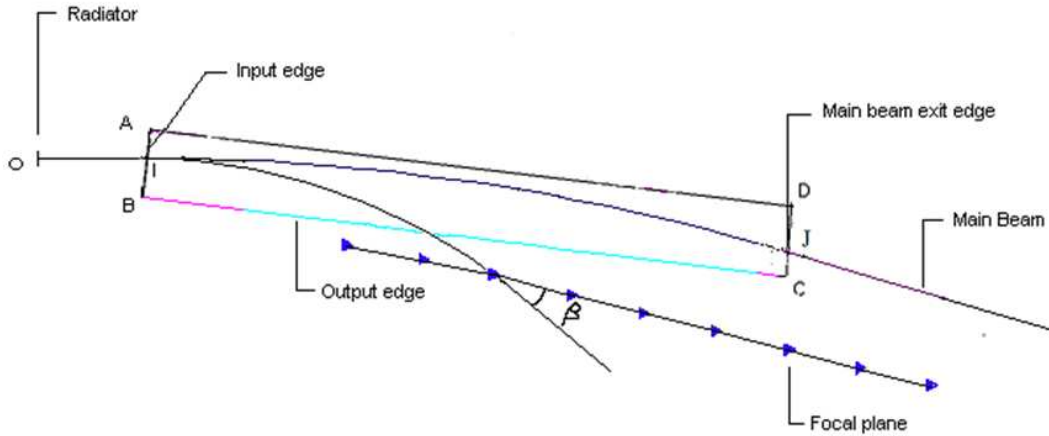
Figure 5.5: Tagger spectrometer geometry used in a TRANSPORT simulation. The magnetic field was modeled with a hard edge approximation. The two parameters which were optimized were the angle between the output edge of the magnet and the beam axis and the horizontal distance from point I and point B (Horizontal shift in the magnet). A field of 1.5 T was assumed.

momentum resolution with the minimum length of the focal plane. As the budget for the magnet is fixed solutions which required much wider poles than the previous design were rejected. The design requirement needed to fulfill the physics goals of GlueX is that the momentum resolution between electron energies of 3 and 11 GeV be better than 0.1%. The resolution is defiend as

$$\mathrm{R} = \frac{\Delta\omega}{\mathrm{D}} \qquad\qquad (5.1)$$

where $\Delta\omega$ is half the radial image size in the focal plane and D is the dispersion.

The best solution found was when the magnet is rotated by 6.5° and the distance from the point where the electrons enter the field to the magnet output edge (I-B in Figure 5.5) is 210 mm. The results of this study compared to the previous best design based on two magnets is shown in Figure 5.6. The point-to-point focus is the location where all electrons of a given energy which start at a single point on the radiator will be focused to a point. The parallel-to-point focus is the point where all particle traveling parallel to each other will be focused to a single point. The focal planes for both point-to-point and parallel-to-point focusing are slightly curved. A straight focal plane has the advantage that the detectors then lie on a line making construction and alignment easier. Therefore a straight focal plane between the other two
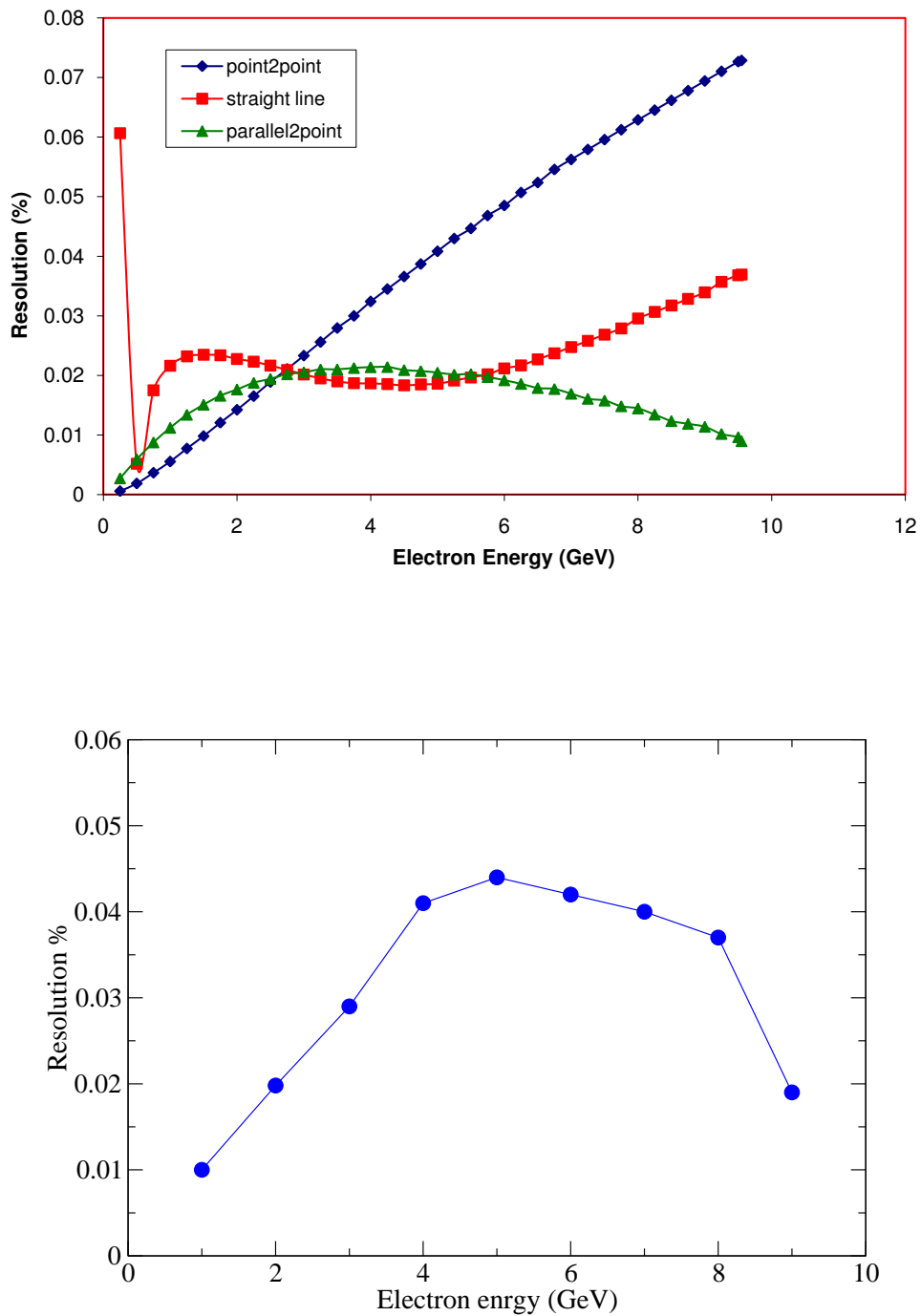
Figure 5.6: The tagger resolution as a function of electron energy as calculated with the TRANSPORT program. The top panel shows the resolution for the new single magnet design and the bottom panel the resolution for the older two magnet design. A 1.5 T field was used for both designs.

options was also studied. In Figure 5.6 the straight focal plane is optimal solution. It has resolution which is fairly flat between 500 MeV and 10 GeV. The resolution is typically between 0.02 and 0.04% of E_0. This is much better than the design requirement of 0.01% of E_0 and is also significantly better than the resolution found in the previous two magnet design.

Based on the very positive results from the TRANSPORT simulations a detailed model of the magnet was developed in TOSCA. This magnet ful-fills the requirements all the requirements listed in the magnet section. Ray tracing calculation were then performed to generate exact numbers for the dispersion and resolution. The results of these calculations are summarized in Table 5.2. In general the resolution is very similar to what was found using TRANSPORT.

At the focal plane, the characteristic bremsstrahlung angle corresponds to a few millimeters of transverse displacement. The vertical beam spot size at the radiator (0.5 mm r.m.s.) contributes a comparable amount because of the large transverse magnification in the dipole transport matrix. However, placing a quadrupole magnet between the radiator and the tagger dipole magnet reduces this magnification nearly to zero over a substantial range of photon energies without substantially changing the other optical properties. Including the quadrupole in the design makes possible a future upgrade of the photon source to employ tagging detectors with two-dimensional readout. The impact of the quadrupole is demonstrated in Figure 5.7. Here 3 GeV electrons were traced through all magnetic fields up to the focal plane. In this study particles were tracked which start with the same angle but different positions on the diamond radiator. The top panel show the trajectories of particle when the quadrupole field is zero. The bottom panel shows the trajectories when the quadrupole is properly adjusted. The quadrupole which will be used is the JLAB QP quadrupole which has a pole tip half aperture of 1.81 cm, an effective length of 31.26 cm, and a maximum gradient of 27 T/m. In this model the distance from the end of the quadrupole to the entrance to the dipole field is 220 cm. The optimum operating gradient was -0.5215 KGs/cm (-5.215 T/m).
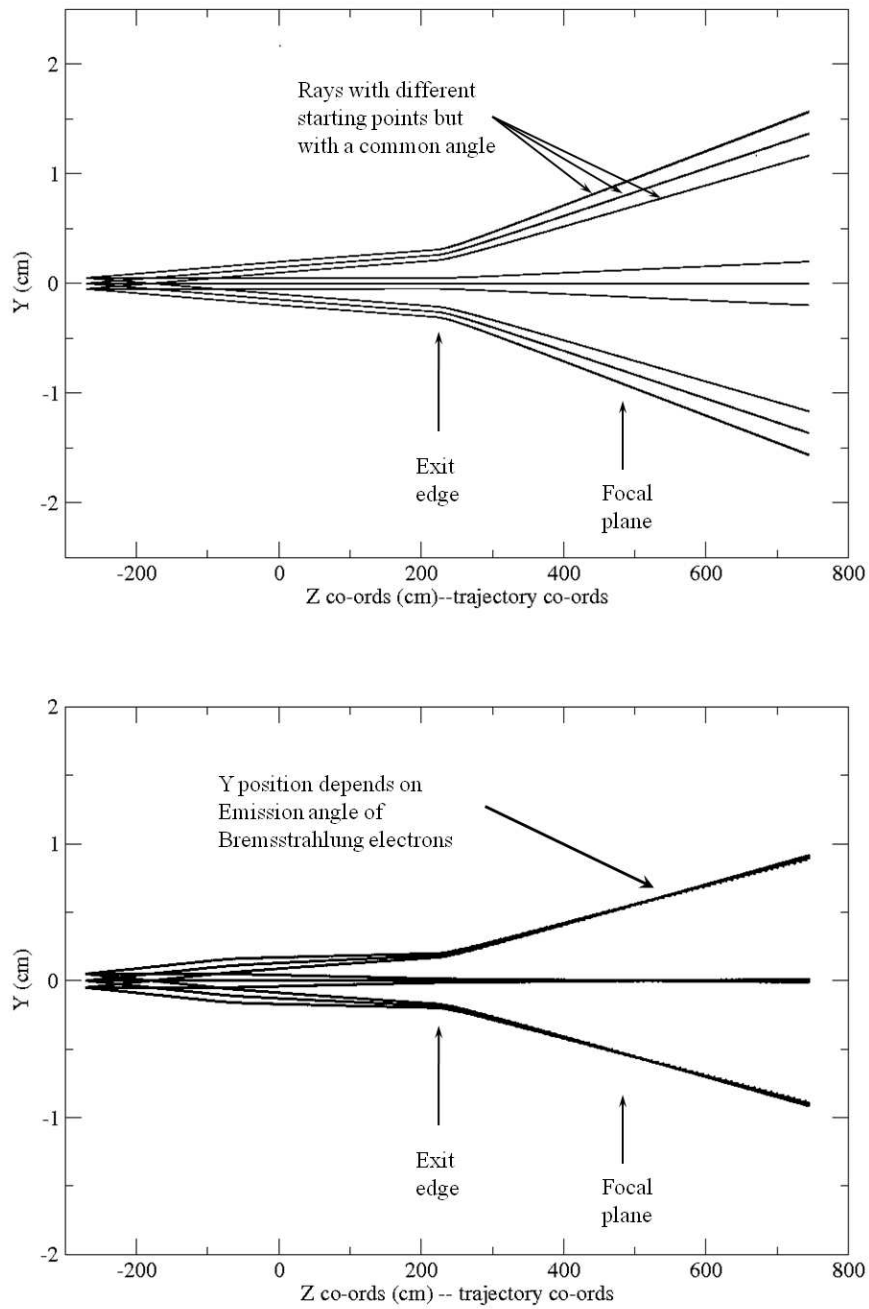
Figure 5.7: The vertical spot size on the focal plane is shown with and without the quadrupole between the diamond radiator and the tagger magnet.

k	(x x)	(y y)	(y y')	Δk_{beam}	Δk_{spot}	Δk_{tot}	Δy_{tot}	y_{char}
(GeV)	(mm/mm)	(mm/mm)	(mm/mr)	($\%E_0$)	($\%E_0$)	($\%E_0$)	(mm)	(mm)
Without quadrupole:								
6	-0.3196	2.1520	19.886	0.080	0.0305	0.0856	1.0760	0.8451
7	-0.2842	2.1072	17.832	0.080	0.0265	0.0843	1.0536	1.0610
8	-0.2444	2.0537	15.739	0.080	0.0235	0.0834	1.0269	1.3378
9	-0.2002	1.9869	13.576	0.080	0.0215	0.0828	0.9935	1.7310
10	-0.1535	1.8966	11.284	0.080	0.0202	0.0825	0.9483	2.3977
11	-0.1265	1.7464	8.657	0.080	0.0157	0.0815	0.8732	4.0472
With quadrupole: (length = 30.126 cm, gradient = -0.52 kGauss/cm)								
6	-0.1934	0.6513	18.921	0.080	0.0212	0.0828	0.3256	0.8041
7	-0.1422	0.5048	16.802	0.080	0.0186	0.0821	0.2524	0.9997
8	-0.0810	0.3032	14.613	0.080	0.0187	0.0822	0.1516	1.2421
9	-0.0054	0.0002	12.299	0.080	0.0202	0.0825	0.0001	1.5681
10	0.0915	-0.5318	9.722	0.080	0.0228	0.0832	-0.2659	2.0659
11	0.1930	-1.8441	6.346	0.080	0.0216	0.0829	-0.9220	2.9666

Table 5.2: Optical properties and resolutions of the tagging spectrometer at the focal plane, for $E_0 = 12 \ GeV$: (x x),(y y),(y y') = first-order transport matrix elements where x and y are radial and transverse coordinates respectively; the focal plane is defined by (x x')=0.; Δk_{beam} = r.m.s. energy resolution due to beam energy uncertainty; Δk_{spot} = r.m.s. energy resolution due to spot size on radiator; Δk_{tot} = total r.m.s. energy resolution excluding detector size; Δy_{tot} = transverse r.m.s. position resolution due to spot size on radiator; y_{char} = transverse size corresponding to one characteristic electron angle $\theta_{Ce} = (m/E_0)(k/(E_0 - k))$.

5.4   Tagger detectors

The Hall-D tagging hodoscope serves the momentum analysis of electrons that scattered off the radiator producing bremsstrahlung photons. The photon energy E_γ is determined as difference between initial electron beam energy (E_0) and energy of the scattered electron (E_e) deflected towards the focal plane. Arrays of scintillation counters along the focal plane allow for detection of scattered electrons with coarse resolution for almost the full energy range and high resolution for energies near the coherent peak. This is realized by instrumentation of two separate detector components:

1. a movable high-resolution device covering the coherent peak, nominally positioned to cover the energy range between 8.5 to 9 GeV (see Section 5.4.1);

2. a coarse resolution device sampling the full energy range from 25% to 97% of E_0 (see Section 5.4.2).

5.4.1   Focal plane microscope detectors

The design energy resolution of 0.1% r.m.s. (see Table 5.2) could be met by non-overlapping detectors which span an energy range of 0.2% each (the r.m.s. deviation of a flat distribution of width W is $W/\sqrt{12} = 0.29W$.) The principal limitation on detector size is imposed by the design goal of tagging collimated photons at rates up to 100 MHz over the coherent peak. The nominal collimated coherent peak has its highest intensity between about 8.5 and 9 GeV (see Fig. 3.3). However, the the tagger sees the scattered electrons for both collimated and uncollimated photons, and the total tagging rate in this region is about twice the collimated rate (see Fig. 3.3), about 200 MHz. If a single phototube can count reliably at 5 MHz, then the energy range detected by a single scintillation counter should be 5 MHz/200 $MHz \times 600 MeV = 15 MeV = 0.12\%$ of E_0. Thus a detector width of 0.1% would satisfy the requirements of both resolution and rate. According to Table **??**, such a detector would have a width of 2.5 mm perpendicular to the electron direction, and detectors for individual channels would be spaced about 17 mm apart along the focal plane.

5.4.2   Fixed focal plane array

Tagging of photons over the full range from 25% to 97% of E_0 is not required as part of the physics program here proposed for GLUEX, but is desirable for two separate reasons. First, it will increase the flexibility of the source

by allowing other possible experiments using highly polarized photons below $8GeV$, or incoherent bremsstrahlung up to $11.7GeV$. This capability is not available elsewhere at JLab, since the Hall-B tagger will not handle beam energies above $6.6GeV$ and the linear photon polarization will be quite low for photon energies above about $4.5GeV$. Second, the process of aligning the crystal radiator for coherent bremsstrahlung requires rotation about several axes and rapid observation of the resulting energy spectra, as described in section 3.7. The low-energy portion of the spectrum, between about 25% and 50% of E_0, is most sensitive to these rotations, and experience with the coherent bremsstrahlung beam at Mainz [17, 18] and in Hall B indicates that the alignment process would be severely compromised if photon energies below $0.5 E_0$ were not measurable. In addition, the high-energy part of the fixed focal plane array can be used as (software) veto in case that more than one electron from a same beam bucket undergo scattering in the radiator with one of them hitting the high-resolution device. In this case the energy balance in the GlueX detector will not match the assumed photon energy detected in the microscope. Photons with energies below the coherent peak do not have to be considered since they would not cause a surplus of longitudinal momentum, which cannot be resolved in a (1C) kinematic fit.

A high energy resolution in the tagger is not deemed necessary for these purposes. A counter width spanning 0.25% of E_0 is considered sufficient in most cases. For operations with an amorphous radiator, these counters would be capable of running a broad-band photon beam with the highest intensities compatible with tagging. Crystal alignment procedures are not carried out at full source intensity, so rate capacity is not a limitation in that application. If a need arose to operate the source in collimated-coherent mode at lower photon energies, for example to obtain increased polarization, then full-intensity operation would always be possible by repositioning the microscope on the focal plane. In this case, the fixed array would be useful in the energy calibration of the movable segment. When used as the primary tagging detectors, the fixed array would be capable of pre-collimated intensities up to 150 MHz/GeV. The initial instrumentation will provide 50% sampling of 60 MeV energy bites below 9 GeV and full coverage of 30 MeV wide counters above 9 GeV photon energy.

5.5 Beam dump optics

Although the full-energy beam leaving the tagger magnet is diverging in both directions, the range of angles is small enough that the beam does not blow up

rapidly. For a dump distance of $30\,m$ the r.m.s. beam size is $6.3\,mm$ horizontal (dominated by the 0.08% beam energy spread) and $0.7\,mm$ vertical (combination of vertical spot size and multiple scattering in a 10^{-4} radiation length radiator.)

These values scale approximately linearly with distance from the magnet to the dump, and are not very sensitive either to the quadrupole or to small rotations of the exit edge of the tagger magnet. Thus the beam dump design is quite insensitive to the beam optics, and depends only on the lateral and longitudinal spread of the shower in the absorber.